

Enhancement Factors: A Central Concept during 50 Years of Surface-Enhanced Raman Spectroscopy

Eric C. Le Ru* and Baptiste Auguie*



Cite This: <https://doi.org/10.1021/acsnano.4c01474>



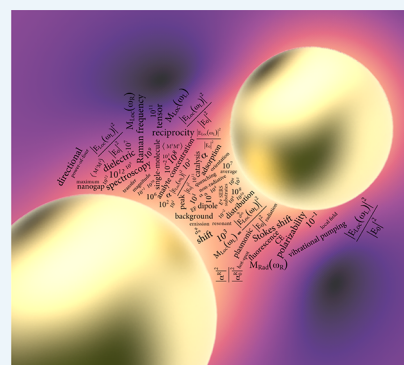
Read Online

ACCESS |

Metrics & More

Article Recommendations

ABSTRACT: In this Perspective, we provide an overview of the core concepts around surface-enhanced Raman spectroscopy (SERS) enhancement factors (EFs), including both theoretical and experimental considerations: EF definitions, the distinction between maximum and average EFs, EF distribution and hot-spot localization, EF measurement and its order of magnitude. We then highlight some of the current challenges in this field, focusing on a selection of topics that we feel are both topical and important: analyte-capture onto a SERS substrate, surface-enhanced resonant Raman scattering, orientation/tensorial effects, and nonradiative effects. We hope this Perspective can provide a platform to reflect on the past 50 years of SERS and its future.



KEYWORDS: surface-enhanced Raman spectroscopy, enhancement factor, hot-spot localization, picocavity

For almost 50 years since the discovery^{1–3} of surface-enhanced Raman spectroscopy (SERS),^{4–6} the concept of a SERS enhancement factor (EF) has consistently been at the forefront of new advances, but also a source of much debate and controversy. The EF is a general term for a quantitative figure of merit describing how much more signal is expected under SERS conditions, using a nanostructured substrate, compared to an “equivalent” Raman experiment without the substrate. At the very start, the observed EF from Raman signals on rough surfaces¹ was clearly incompatible with a simple explanation in terms of increased surface area (an EF of 10–100 at most), and this provided the impetus to seek other explanations to describe the giant enhancements. Such effects were quickly identified as electromagnetic in origin:^{2,3} the local field enhancement due to plasmon resonances in metallic nanostructures.^{7,8} Then, in the 1990s, estimates of the EF were central to the development and interpretations of single-molecule SERS, with much debate in the 2000s—and still to this day—on what the maximum achievable electromagnetic enhancements are.⁹ Today, the concept of EF is still central to current surface-enhanced spectroscopy research, from the harder-to-explain EFs recently reported in SERS research on picocavities,¹⁰ to efforts to understand the various mechanisms contributing to plasmonic photocatalysis.¹¹ More pragmatically, the EF is one of the most important metrics for any practical

application of SERS.^{12–14} Indeed, for many newcomers to the field, it is often their first question: Which EF can I expect? And the answer is, as often in such cases, “well, it depends ...”

In this Perspective, we first summarize the core definitions and concepts around SERS EFs and then highlight several specific aspects of SERS EFs that have arisen from the more recent research: (i) the importance of analyte transfer to the SERS substrate, (ii) SERS EFs for resonant molecules (dyes), (iii) orientation effects, and (iv) nonradiative processes in SERS and surface-enhanced reaction/catalysis. The aim is not to be exhaustive, nor even to provide a review of the recent research in these areas. Instead, we focus on simple examples and try to discuss the implications in terms of future research and applications.

CORE CONCEPTS REGARDING SERS EFs

There are many different ways to define SERS EFs, depending on the point of view (theory/calculation vs experiment/

Received: January 30, 2024

Revised: March 12, 2024

Accepted: March 20, 2024

measurement) and the availability of parameters (substrate geometry, number of adsorbed molecules, orientation, etc.).^{4,9,14} Theoretical calculations in particular can easily assume an idealized comparison between signals obtained with and without a substrate near the molecule of interest, while, of course, actual measurements introduce many additional complications.

Theoretical Definitions. The simplest theoretical approach is based on a classical description of the Raman process, in terms of an empirical Raman polarizability α_0^R , which determines the strength of the induced Raman dipole p_0 for a given incident field E_0 at the molecule position (Figure 1).¹⁵ The same applies under

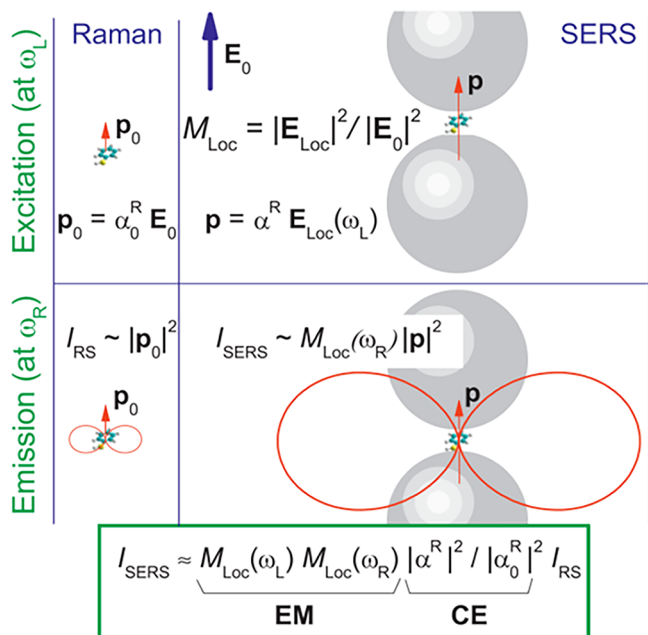


Figure 1. Schematic representation of the main mechanisms at play in SERS, based on the classical electromagnetic theory of a polarizable Raman dipole (ignoring most tensorial/orientation effects). In standard Raman scattering, the induced Raman dipole p_0 is proportional to the electric field at the dipole position E_0 and its emission (the Raman signal) is proportional to $|p_0|^2$. In SERS, the incident field at the molecule position is different, E_{Loc} (usually larger in magnitude), and the emitted intensity is also modified (usually enhanced). Both of these effects are multiplicative and give rise to the electromagnetic (EM) EF. The Raman polarizability α^R may also be modified giving rise to an additional term corresponding to the Chemical Enhancement (CE) factor. [Reprinted with permission from ref 15. Copyright 2013, Springer Nature.]

SERS conditions (for a molecule adsorbed or close to a metallic nanostructure), but both the polarizability α^R and local field E_{Loc} may be modified by the presence of the metallic object. In addition, the emission properties of any dipole in the vicinity of the surface are also modified, which further affects the emitted SERS intensity, giving an overall enhancement factor EF, which is given by

$$EF = M_{Loc}(\omega_L) M_{Rad}(\omega_R) \frac{|\alpha^R|^2}{|\alpha_0^R|^2} \quad (1)$$

The first term is the local field enhancement factor at the incident laser frequency ω_L :

$$M_{Loc}(\omega_L) = \frac{|E_{Loc}(\omega_L)|^2}{|E_0|^2} \quad (2)$$

The second term is the dipole radiation/emission enhancement factor at the Raman frequency ω_R . It turns out that due to optical reciprocity, this enhancement factor can, in many situations, be approximated by the corresponding local field enhancement factor:¹⁶

$$M_{Rad}(\omega_R) \approx M_{Loc}(\omega_R) \quad (3)$$

The equality would only be true under fairly restricted conditions, but the approximation remains valid (at least for order-of-magnitude estimates) in the majority of situations relevant to SERS.¹⁶ These first two terms arise from the electromagnetic influence of the metal substrate on the molecule and are often referred to as the electromagnetic (EM) enhancement. It is also common to neglect the Raman Stokes shift and assume that $M_{Loc}(\omega_R) \approx M_{Loc}(\omega_L)$, which results in the so-called E^4 -approximation for the EM EF:

$$M_{Loc}(\omega_L) M_{Rad}(\omega_R) \approx \left(\frac{|E_{Loc}(\omega_L)|}{|E_0|} \right)^4 \quad (4)$$

It is important to emphasize that this power-of-four law relates to the field ratio or enhancement $|E|/|E_0|$, not to the incident field itself, and is therefore independent of incident laser power. The dependence of the SERS intensity with incident power therefore remains linear (as for the Raman intensity), not quadratic. Note also that the above description has ignored for simplicity the complications associated with the tensorial nature of the Raman effect, the orientation of the molecules, or the polarization of the field.⁴

The third term in eq 1 relates to the change in molecular properties (for example, conformation, charge, electronic resonance, or new charge transfer resonances) as a result of direct adsorption or just proximity to the surface and is usually referred to as Chemical Enhancement (CE). Note that some authors prefer to reserve this term for molecules that are chemisorbed to the surface. We also note that the strict separation between EM and CE as in eq 1 is an oversimplification, for example, if charge transfer states are involved.^{17,18} In any case, the main characteristics of the CE contribution is that it is highly molecule-dependent whereas the EM applies (in a first approximation) similarly to all molecules.¹⁹ For this reason, one could argue (probably controversially) that the CE is an unwanted distraction in describing the general mechanism of SERS. When focusing on the EF properties of a SERS substrate, independent of the analyte, one would wish to study molecules that are not subject to CE so that results and interpretations retain a general validity for all molecules. This is easier said than done as many molecules are affected in one way or another by the proximity of the metal surface. This often-unavoidable interplay between substrate and analyte therefore justifies the continuous efforts of the research community to understand the many facets of the CE.^{19,20} This has also motivated new experimental approaches to remove or reduce CE, notably, the use of a very thin dielectric layer on top of the metal surface (a scheme called SHINERS, which stands for Shell Isolated Nanoparticle Enhanced Raman Spectroscopy).²¹

Average, Maximum, and Distribution. The previous definition relates to the theoretical EF experienced by one molecule at a well-defined position. In practical situations, we

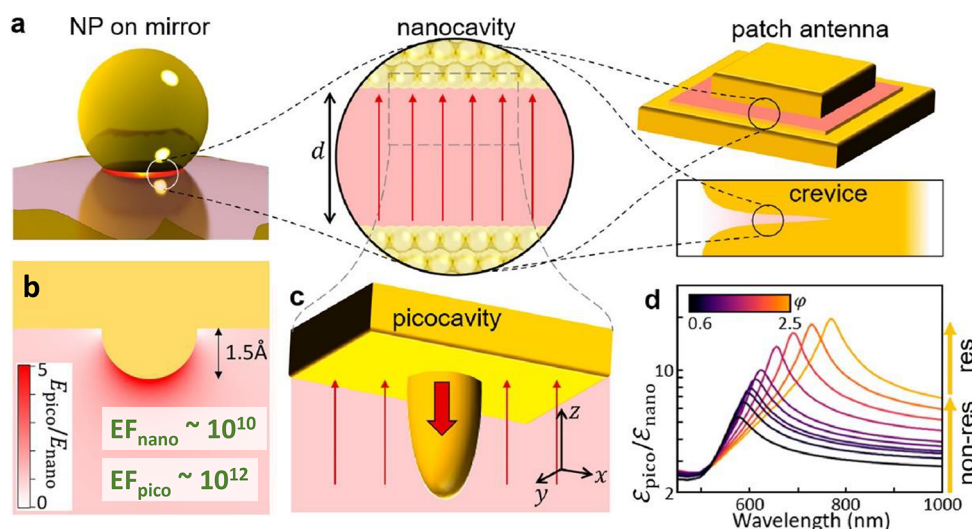


Figure 2. Principles of a picocavity:¹⁰ (a) a nanogap or nanocavity, commonly used in SERS, can be formed in a patched antenna, at the crevice between two nanoparticles or between a particle and a flat surface. The SERS EF in a nanocavity can reach 10^{10} . (b, c) A picocavity is formed inside a nanocavity by a single gold atom protruding off the surface (possibly dynamically). This provides an additional field enhancement, which (d) depends on the aspect ratio ϕ , and (b) is extremely localized around the protuberance. This mechanism is believed to further push SERS EFs up to 10^{12} , but only over a region of a few Ångströms. [Adapted with permission from ref 10. Copyright 2022, American Chemical Society, Washington, DC.]

have many molecules at different locations on the surface where the field enhancements can differ widely, which is further magnified for the EF by the fourth-power dependence. As a result, most SERS substrates present a distribution of SERS EFs, and more often than not, a very wide (typically long-tailed) distribution where the maximum and minimum EFs differ by many orders of magnitude.^{22,23} The regions of maximum enhancements, called hot spots, largely dominate the measured SERS signal.²⁴ They are, for example, located in the gap between two nanoparticles²⁵ or a nanoparticle and the substrate, or at the tips of elongated particles like nanorods. These hot spots are moreover highly localized,²⁶ with typically a rapid dropoff by 1 order of magnitude or more from the location with the highest EF to a position just a few nanometers away.²⁷ This strong localization of EFs on position greatly influences the statistics of SERS signals as they can be dominated by small regions that may contain only a few or, indeed, even a single molecule.²⁸ It also contributes to the high nonuniformity of SERS signals.¹⁴

The full probability distribution of EF gives maximum information about a SERS substrate, but in practice, we can often focus on two simple metrics:^{22,23} (i) the surface-average EF, $\langle \text{EF} \rangle$, which relates to the overall SERS signals for a uniform molecular coverage; and (ii) the maximum SERS EF, EF_{max} , which relates to the largest signals that could be detected from a single molecule precisely located at the position of highest enhancement (hot spot). Note that single-molecule experiments require special techniques, such as the bianalyte SERS method,²⁴ ideally using isotopologues,^{29,30} to demonstrate the single-molecule nature of the signals. Because of the strong hot-spot localization, EF_{max} is often as much as 100 to 1000 times larger than $\langle \text{EF} \rangle$. As a rule of thumb, the larger the maximum EF, the more localized the hot spot; therefore, for applications requiring good signal stability and reproducibility, substrates with lower but more uniform EFs should be preferred. This can be typically achieved by avoiding nanogaps and sharp tips/edges.³¹

Another mechanism in the formation of hot spots has also more recently emerged, initially from tip-enhanced Raman spectroscopy (TERS) experiments,³² where the metallic tip of

a scanning tunneling microscope is used to dynamically form a SERS substrate by creating a nanogap. The main advantage of this approach is its mapping ability. In ultrahigh vacuum experiments, it has been shown that the resolution of the technique can reach the subnanometer range (a few Ångströms),^{33–35} suggesting the existence of even more highly localized hot spots. A similarly high hot-spot localization was also evidenced with the Nanoparticle-over-Mirror (NPoM) approach.^{36–38} In both cases, it has been argued that the hot spot is formed by the presence of a single Au atom (which may move dynamically over time) closer to the other surface, to form a so-called picocavity¹⁰ (Figure 2). On top of the tighter localization, the SERS EFs at the hot spot of a picocavity could be higher by ~ 100 than in a standard gap hot spot and reach 10^{12} . The theoretical modeling of such picocavities is beyond the classical model presented here, but new approaches have been developed to explain such effects.^{39,40}

Experimental Definitions. The definitions discussed so far are well-suited to theoretical calculations, but do not easily translate to experiments. The most common definition in this context is the SERS substrate EF:

$$\text{SSEF} = \frac{I_{\text{SERS}}/N_{\text{SERS}}}{I_{\text{Raman}}/N_{\text{Raman}}} \quad (5)$$

where I_{SERS} and I_{Raman} are the measured SERS and Raman intensities for the same analyte measured under identical conditions and N_{SERS} and N_{Raman} are the number of molecules producing the signal in each case. The advantage of this definition is that it aligns well with the theoretical definitions earlier and should match the average SERS EF $\langle \text{EF} \rangle$ in the absence of Chemical Enhancement. The main disadvantage is that it is difficult in practice to reliably estimate N_{SERS} and N_{Raman} , even within an order of magnitude, as discussed, for example, in refs 9 and 14. I_{Raman} may also be difficult to measure for resonant molecules like dyes where fluorescence overwhelms the Raman signal, but not the SERS, thanks to fluorescence quenching by the metal.⁴¹

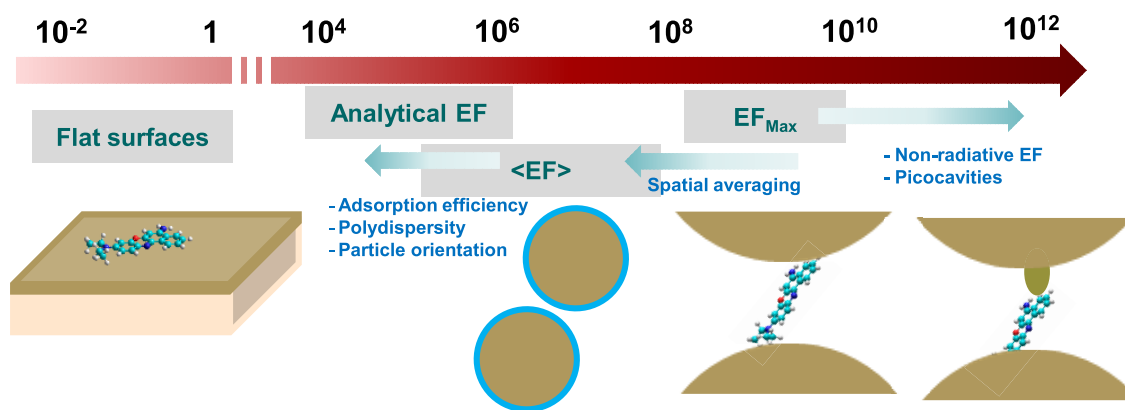


Figure 3. Schematic illustration of the typical magnitude of SERS EFs.

A more pragmatic and practical alternative can be used for SERS of analytes initially in solution or gas phase, the analytical enhancement factor (AEF):

$$\text{AEF} = \frac{I_{\text{SERS}}/c_{\text{SERS}}}{I_{\text{Raman}}/c_{\text{Raman}}} \quad (6)$$

where c_{SERS} and c_{Raman} are now the analyte concentrations used during preparation. The AEF can easily be determined and is more closely relevant to experiments with this particular analyte. However, the results are much more analyte-dependent, as they do not account for the critical step of the transfer of analyte from solution to surface, for example, the adsorption efficiency for colloidal substrates. Even for 100% adsorption, the AEF tends to be much smaller than the theoretically predicted (EF), because of substrate orientation averaging, molecule orientation averaging, and polydispersity in the substrate (e.g., colloids).

Finally, we note that these experimental EFs (SSEF and AEF) measure the overall SERS EF, which includes both electromagnetic and chemical contribution, with the latter potentially contributing to large differences between different analytes. Orientation effects (discussed later in this paper) might also add to these analyte-to-analyte variations. This makes a direct comparison of experimental EFs difficult, unless measured with the same analyte/metal combination. One should ideally choose an analyte with either a small CE contribution or at least a well-defined CE EF, together with a well-defined and characterized orientation on the surface. Unfortunately, no consensus has yet been reached on which analyte(s) should be used for this purpose. Reference 14 proposed a first step in this direction by considering the respective advantages of common SERS analytes with high affinity for gold and silver, but more work is needed to study their potential CE and orientation effects.

The Order of Magnitude of the SERS EF. Given the many possible definitions of SERS EFs, it is not surprising that a wide range of SERS EFs magnitudes have appeared in the literature, from as low as 10^{-2} (quenching rather than enhancement) to as high as 10^{15} . This can be confusing and intimidating for newcomers to the field. The SERS EF scale is illustrated schematically in Figure 3, and the main points discussed below.

- The predicted and measured (using single-molecule SERS) EF_{max} for typical substrates is in the range of 10^8 – 10^{10} , the upper end corresponding to substrate with nanogaps or sharp edges or tips.^{9,42,43}
- Values for the single-molecule EF_{max} of 10^{14} – 10^{15} were artificially inflated by using resonant analytes for SERS, but nonresonant cross sections for the Raman refer-

ence.^{44,45} They do not correspond to any of the definitions we have discussed here and are misleading, but have unfortunately lingered in the literature.

- The average EFs (or SSEFs) are typically of the order 10^5 – 10^8 ,^{46,47} or ~ 100 – 1000 times less than the maximum EFs due to hot-spot localization.
- The Analytical EFs (AEFs) are typically of the order of 10^4 – 10^6 , or ~ 10 to 100 times less than average EFs, due to 3D-2D analyte transfer, orientation averaging, colloidal polydispersity or substrate imperfections, etc.^{9,13,14}
- At the lower end of this scale, we can mention the EF on flat metallic surfaces, which can be as low as 10^{-2} : in fact, quenching and resonant molecules such as dyes at high coverage are usually necessary to detect a SERS signal.⁴⁸ The flip side is that the EF, in this case, is perfectly uniform and it is an ideal model system to test more advanced concepts such as surface-selection rules.⁴⁹
- As we will discuss later in this work, for phenomena like vibrational pumping,⁵⁰ the relevant SERS cross-section is dominated by nonradiative effects, which can further boost the maximum EF to $\sim 10^{12}$.⁵¹
- There is evidence that the maximum EF in picocavities (ultralocalized hot spots) could be 100 times larger than in the nanocavity supporting them and reach $\sim 10^{12}$.¹⁰

Finally note that we have ignored any CE in this discussion and this could add a molecule-dependent factor of typically between 10^{-1} and 10^2 on top of these EM EFs.¹⁹

Another point worth noting is that single-molecule detection is often used as an argument for how good SERS is, or how good a SERS substrate is. This is not quite true in general. Using one of the most efficient and most emblematic SERS analytes, Rhodamine 6G, excited at 514 nm, it is, in fact, possible to demonstrate single-molecule detection at very low SERS EF, on the order of 10^4 only at the molecule position.⁵² This is because, thanks to the resonant Raman effect, the Raman cross-section is then on the order of 10^{-24} cm²/sr.⁵³ A modest 10^4 EF is sufficient to push it up to 10^{-20} cm²/sr, which is comparable to fluorescence cross-section once taking into account the much broader fluorescence spectrum compared to a Raman peak (a factor of ~ 100). In contrast, single-molecule SERS with nonresonant molecules with cross sections $\sim 10^{-30}$ cm²/sr, which would be much more broadly applicable, does require large EFs, on the order of 10^{10} .⁴³

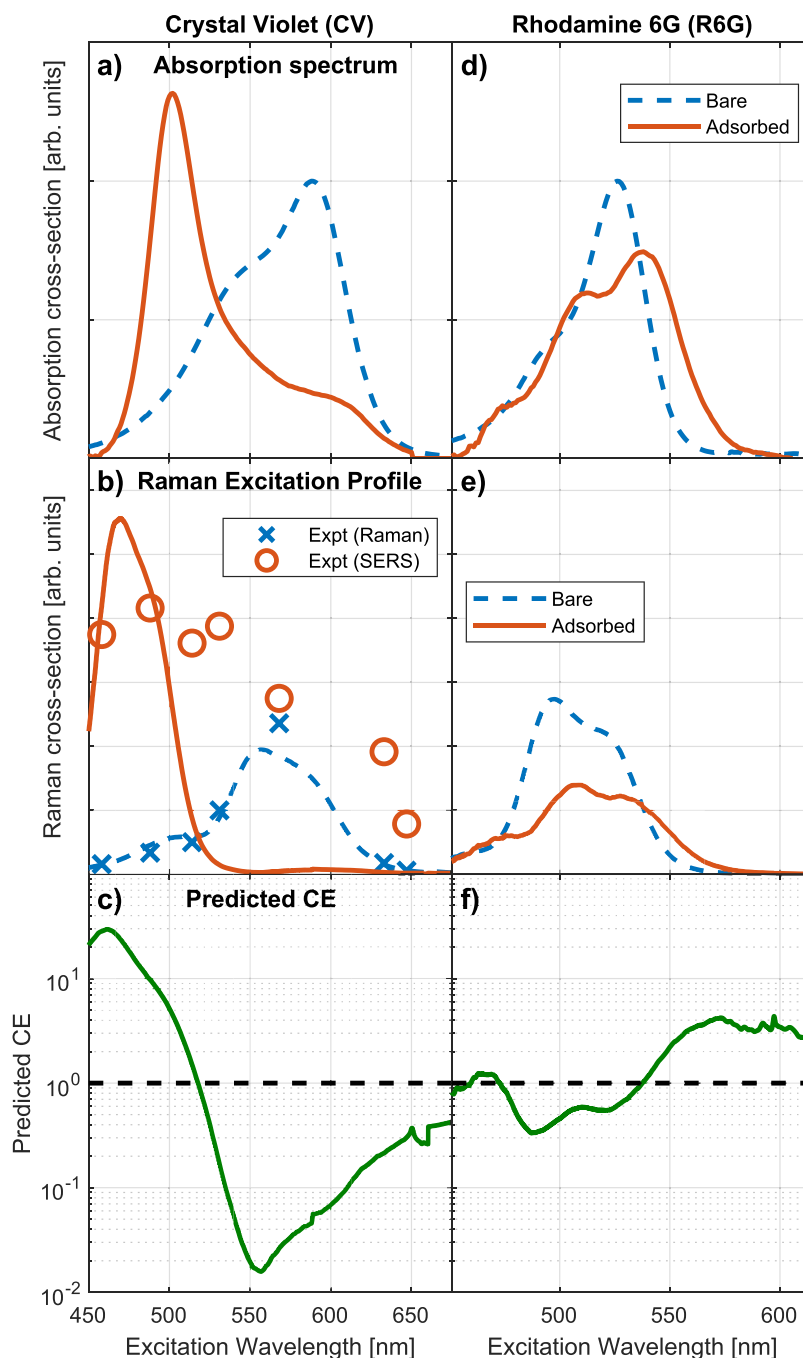


Figure 4. Summary of effects related to adsorption-induced shifts in the molecular resonances of dyes for Crystal Violet (left) and Rhodamine 6G (right). (a, d) The absorption of the adsorbed dyes is compared to that of the bare dye in water. See ref 64 for details of these measurements. (b, e) The absorption spectra are used to predict Raman excitation profiles for the bare and adsorbed dyes, following the model in refs 65 and 66. Although a number of approximations are made in this model, the prediction agrees reasonably well with previous measurements of the CV bare cross-section.⁶⁷ The predicted shift in SERS REP is also supported by experiments.⁶⁸ (c, f) The predicted CE resulting from these absorption shift is computed from the ratio of adsorbed to bare REPs. Even for a modest shift as for R6G, non-negligible CEs are predicted (see panel (f)).

A SELECTION OF TOPICAL CONSIDERATIONS REGARDING SERS ENHANCEMENT FACTORS

SERS is a Surface Spectroscopy. The title of this section may appear to be stating the obvious, but it emphasizes some simple yet important consequences, in terms of SERS potential applications. Imagine an analyte in solution with no particular affinity to the SERS substrate, say a silver island film with an average SERS EF of 10^5 for the sake of example. As we dip the substrate in the solution, we will measure the SERS signal of only

the molecules in the closest vicinity, say within 2 nm. We could alternatively measure the same solution with the same microscope objective with normal Raman and would then detect the unenhanced Raman signal of the molecules over the full depth of the scattering volume, say $200\ \mu\text{m}$ (note this is objective dependent), so 10^5 times more molecules. This has the same effect as the average 10^5 SERS EF and the two signals are the same! This highlights one crucial aspect of SERS applications: the SERS EF is only useful if we have an efficient method of transferring the target analyte to the surface (typically

from a solution or gas). This is why SERS also typically only targets low concentrations, as for typical colloidal or dry substrates, the available surface area is quickly saturated (at concentrations of the order of 1 μM). Adding more molecules would not increase the SERS signal much.

This necessary 3D-to-2D transfer can be a challenge as it is typically very case-dependent (analyte and type of substrate). But it is also an opportunity as innovative approaches to this transfer can really unlock the full potential of SERS for applications, for example by preconcentrating the analyte on the SERS substrate. The standard method of drying a drop of analyte solution on top of a SERS substrate achieves that, but with poor uniformity and control. The use of superhydrophobic surfaces can dramatically enhance that approach, with gains of the order of 10^2 – 10^3 reported in average signal or lower detection limits.^{54–58} These do not correspond to any change in SERS EF, but simply to a more efficient analyte transfer. Another approach is to ensure selective binding of the target analyte to the SERS substrate.^{59,60} A further improvement in this step is to devise schemes to restrict analyte adsorption to only the hot spots,^{61–63} which not only increases the measured average EF, but also reduces the SERS fluctuations.⁶³

The Difficulties with SERS EFs for Resonant Molecules.

Historically, dyes have played and still play an important role in the development of SERS. As hinted at already, their much larger Raman cross-section thanks to the Resonance Raman (RR) effect, provides a huge boost in SERS signal (then often called SERRS), compared to nonresonant molecules on the same substrate, potentially by as much as 10^6 . It is therefore no surprise that they are often preferred in SERS experiments. This would be fine if the results from dyes could translate easily to nonresonant molecules. However, it has been shown^{64,69} that the electronic resonance of dyes can be subject to shifts induced by the proximity of the metal surface. Because of the resonant nature of the RR effect, a small shift in resonance can result in a large change in the Raman polarizability,⁷⁰ as we will show explicitly below. This modification qualifies as a Chemical Enhancement effect (third term in eq 1) and it is very molecule-dependent.

This is illustrated in Figure 4 for two common SERRS analytes, Crystal Violet (CV) and Rhodamine 6G (R6G), adsorbed on silver nanoparticles.⁶⁴ The case of CV is fairly clear-cut: there is a large shift in the electronic resonance from 590 nm for free CV down to 500 nm for adsorbed CV (Figure 4a). Such a large shift must be due to a chemical change in the adsorbed molecule, possibly related to charge/protonation (CV is a known pH indicator). The Raman excitation profile (REP), which quantifies the strength of the Raman signal as a function of excitation wavelength, can be expected in a crude approximation to be similar to the electronic absorption spectrum. More quantitative predictions of the REP can in fact be made following the model presented in refs 65 and 66. This prediction is shown in Figure 4b and compared to measurements of the Raman cross-section of CV,⁶⁷ showing that the agreement is reasonable. From the point of view of SERRS of CV, the absorption shift evidenced in Figure 4a should have a similarly large effect on the adsorbed CV Raman cross-section. The REP model predicts that it should indeed peak at ~ 470 nm, instead of 565 nm (Figure 4b). The ratio between the predicted REP in SERRS and Raman correspond to the predicted chemical enhancement for CV (shown in Figure 4c), as a consequence of this metal-induced absorption shift. Given the large absorption and REP

shifts, large variations in CE are predicted with excitation wavelengths, over more than 3 orders of magnitude.

To find further experimental evidence for this, the SERRS intensity of the 1620 cm^{-1} peak of CV adsorbed on unaggregated silver nanoparticles was measured at varying excitation wavelengths.⁶⁸ This intensity is proportional to the adsorbed CV Raman cross-section $d\sigma_{\text{ad}}/d\Omega$ but also to the intrinsic EM SERS EF:

$$I_{\text{SERS}}(\lambda_{\text{L}}) \propto \text{EF}(\lambda_{\text{L}}) \frac{d\sigma_{\text{ad}}}{d\Omega}(\lambda_{\text{L}}) \quad (7)$$

In order to remove this intrinsic wavelength-dependence of the EM SERS EF, a nonresonant molecule, bipyridine ethylene (BPE) was also measured under identical conditions. $\text{EF}(\lambda_{\text{L}})$ is then deduced using the 1605 cm^{-1} peak of BPE, assuming that BPE does not exhibit any wavelength-dependent CE. The derived $d\sigma_{\text{ad}}/d\Omega$ for adsorbed CV is also shown in Figure 4b and clearly shows a marked shift in resonance toward the blue, in good agreement with the measured blueshift in absorption. It is worth pointing out that the interpretations of ref 64, in terms of absorption shifts, have been questioned in ref 71 but the dye concentrations were much higher there and the differential absorption spectra most likely dominated by dye-induced colloid aggregation. The additional SERS REP results presented here further support the modified absorption interpretation of ref 64.

In the case of Rhodamine 6G (Figures 4d–f)), the adsorption-induced shift is relatively modest, suggesting that the dye does not interact strongly with the silver surface. Yet, the REP predictions for such a shift still indicate that wavelength-dependent CE factors between 0.3 (~ 500 nm) and 4 (> 570 nm) could result. Another interesting feature (not shown here) is that the optical absorption is concentration-dependent, suggesting that the EM interaction between R6G dyes on the surface can affect their optical absorption, even at very low coverage.^{64,72} This is similar to the formation of dye dimer/aggregates. One would expect that such interactions would also affect their SERS properties but this has not yet received much direct experimental investigation.⁶⁹

The Importance of Orientation Effects. The importance of molecular orientation, substrate orientation, and polarization effects in SERS have been recognized very early on and discussed under the general umbrella of SERS selection rules.⁴⁹ These are well-explained by classical EM theory,^{4,73} and their effect has been evidenced experimentally in simple cases such as planar surfaces.⁴⁸ In more realistic and less controlled situations, it remains a challenging problem for several reasons: the molecular orientation on the surface is usually not well-known; the substrate geometry itself is not clearly defined, especially if roughness is involved; nanoparticles in solution are typically randomly oriented; and the Raman tensor of the vibrational modes may change upon adsorption. As with CE, these effects are highly molecule-dependent. Due to these complications, such orientation effects are often neglected in theoretical calculations of SERS EFs or when comparing numerical predictions with experiments. We have done the same in this Perspective, ignoring tensorial and orientation effects in our introduction to SERS EF and in the discussion so far. This is however potentially a huge problem as orientation effects are a major contributing factor in the SERS EF. Like the CE, we would like to ignore them to get more general applicability, but like the CE, they appear to affect most molecules, enough that they should not be ignored. From the early days, it was

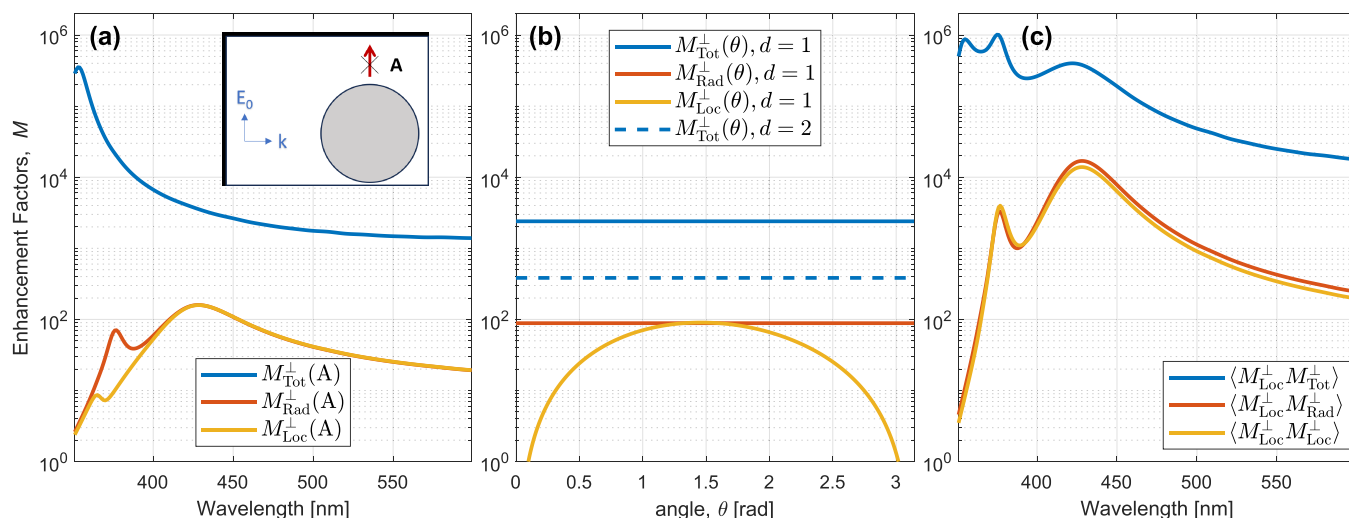


Figure 5. Illustration of predicted nonradiative enhancement factors for the model system of a 60-nm-diameter silver nanoparticle in water, from extensions of Mie theory for dipole emission.^{4,78} (a) Wavelength dependence of the local-field EF, M_{Loc}^{\perp} , radiative decay rate EF, M_{Rad}^{\perp} , and total decay rate EF, $M_{\text{Tot}}^{\perp} = M_{\text{Rad}}^{\perp} + M_{\text{NR}}^{\perp}$, for a dipole perpendicular to the surface at point A at a distance of $d = 1$ nm from the surface (see inset). M_{Loc}^{\perp} and M_{Rad}^{\perp} are comparable due to optical reciprocity.¹⁶ M_{NR}^{\perp} largely dominates M_{Tot}^{\perp} . (b) Position dependence of these EFs for a fixed wavelength of 458 nm. Note that the decay rate EFs are, by definition, not position-dependent (but M_{NR}^{\perp} strongly depends on d). (c) Surface-averaged EFs for standard SERS EF, $\langle M_{\text{Loc}}^{\perp} M_{\text{Loc}}^{\perp} \rangle \approx \langle M_{\text{Loc}}^{\perp} M_{\text{Rad}}^{\perp} \rangle$, and for nonradiative SERS EF, $\langle M_{\text{Loc}}^{\perp} M_{\text{Tot}}^{\perp} \rangle$, neglecting the Stokes shift.

recognized that the EF along the parallel component to the surface was much smaller than along the perpendicular direction. Calculating the EF for a general orientation and polarization can be complicated,^{73–75} so we can instead calculate EFs for the two extreme cases of fully in-plane or fully out-of-plane uniaxial Raman tensors. In the model case of a silver sphere in water at resonance (430 nm), the average perpendicular SERS EF $\langle M_{\text{Loc}}^{\perp} M_{\text{Loc}}^{\perp} \rangle$ is ~ 20 times larger than its in plane counterpart $\langle M_{\text{Loc}}^{\parallel} M_{\text{Loc}}^{\parallel} \rangle$. For a less-symmetric substrate, such as a dimer of nanoparticles, we can moreover consider either a fixed incident polarization or random orientation, which adds another factor of ~ 1 order of magnitude.⁷⁵ Clearly, both orientation and polarization can therefore have a large effect on the overall SERS EFs, often comparable with what we expect from CE. Although these can be studied in careful experiments,^{72,74–77} they nevertheless add another layer of complication for the general applicability of SERS.

Nonradiative Effects and Surface-Enhanced Catalysis.

As SERS and plasmonics continue to progress and evolve, new phenomena are being explored where conventional definitions of SERS EFs may no longer be suitable. Let us discuss two topical examples. The first one is SERS vibrational pumping,^{50,79} which has recently received renewed attention in the context of the optomechanical model of SERS.^{36,80,81} In a nutshell, under some high-EF conditions, the SERS cross-section may be large enough to generate Raman events, which excite the molecule to a higher vibrational mode, at a faster rate than the relaxation time of these vibrational excitations (vibrational lifetime). In this case, the vibrational mode population should increase beyond its thermal equilibrium value, and this can be observed as an increase in the anti-Stokes SERS signal or in the anti-Stokes to Stokes ratio.^{50,79} There is conclusive evidence that vibrational pumping does occur in SERS and the SERS EF can even be inferred from such measurements, but it tends to be higher than the one inferred from a standard SERS measurement.^{9,51,82} We can reconcile this discrepancy: for an emitter on a metal surface, we have so far only discussed the possibility of enhancing its radiation (a photon is emitted and detected in the far-field),

through the factor M_{Rad}^{\perp} . There is always in parallel the possibility of emitting a photon that is absorbed in the metal substrate, i.e., nonradiative emission.⁴ For molecules adsorbed on a metal surface, this nonradiative channel is typically much larger than the radiative one; this is why fluorescence is quenched as the two decay channels compete with each other.⁸³ In SERS or Raman, there is no decay from an excited state as it is a scattering event, so the nonradiative channel occurs in parallel to the nonradiative ones, i.e., there is no competition. In the majority of situations, this nonradiative decay is irrelevant since it is not observable as a SERS signal by a detector. But these events do occur and affect the molecule, for example, contributing to vibrational pumping. This explains why the SERS EF in vibrational pumping should be larger. Theoretical predictions for this effect should not assume the $|E|^4$ approximation (eq 4), but instead compute the total decay rate enhancement factor M_{Tot}^{\perp} , typically dominated by the nonradiative component M_{NR}^{\perp} .^{4,83,84} This EF can also, in principle, be inferred experimentally from comparing the SERS and surface-enhanced fluorescence EFs.⁸⁴ The nonradiative SERS EF is then given by $M_{\text{Loc}}^{\perp}(\omega_L)M_{\text{Tot}}^{\perp}(\omega_R)$. Examples of predicted SERS radiative and nonradiative EFs are summarized in Figure 5 for the model system of a silver nanoparticle in water. The nonradiative SERS EF is highly distance-dependent, and can be up to 100 times larger than the standard SERS EF.⁸⁴ Related to these effects is the common observation alongside SERS peaks of a so-called SERS background, which may be attributed to residual fluorescence^{85,86} or plasmonic luminescence.⁸⁷ In such cases, the SERS background can be used to study the local field^{85–87} and nonradiative⁸⁴ enhancement factors.

Similar considerations can be made in the context of surface-enhanced catalysis or plasmonic-enhanced reaction.¹¹ Several mechanisms are being considered to explain such results.^{11,88–91} Some are based on simple optical absorption by the catalyst or molecule, so they should be characterized by the enhancement factor for absorption, typically M_{Loc}^{\perp} . This is, for example, the case for enhanced photobleaching of dyes on metal surfaces.⁹² In other cases, it is believed that reactions are photoenhanced by

the creation of hot electrons in the metal, as a result of localized surface plasmon excitation.^{11,88,89} Such effects should then be characterized by yet another enhancement factor, related to optical absorption in the metal structure (which is different to the EF for the field outside its surface). One should also aim to measure the enhancement of the reaction yield but this is a difficult endeavor. Finally, reactions could also be surface-enhanced, as a result of intense vibrational pumping (for example, resulting in the destruction of the molecule).⁸¹

OUTLOOK

Arguably, despite all the excitement about SERS over the last 50 years, which was often carried by the prospect for large enhancement factors, SERS has not yet delivered on its promise to revolutionize analytical chemistry. Some of the reasons for this have been hinted at in this Perspective: (i) only molecules on the surface are enhanced, which probably precludes SERS from ever reaching the same broad range of applicability as Raman or IR absorption; and (ii) chemical enhancements and orientation/polarization effects render the results highly molecule-dependent, which has hindered progress in our understanding of the technique. But these drawbacks (in terms of the general applicability) are also advantages from many other perspectives. SERS remains a technique with unparalleled sensitivity to the properties of molecules on surfaces. Combined with techniques of selective and targeted binding, it should be able to deliver reliable and reproducible detection of molecules of interests, down to the single molecule level. But some work is needed to optimize the surface/analyte interaction for each new target molecule. SERS also remains the method of choice for studying and monitoring the properties of molecules on surfaces, from electrochemical to catalytic reactions. Looking further ahead, there is an increased interest in all-dielectric nonmetallic structures supporting SERS.^{93,94} Although EFs may be smaller, this could be more than compensated by the potential for these structures to be three-dimensional. Perhaps such a porous structure could solve many of the 3D-to-2D transfer issues and also have general applicability. Even with an average SERS EF of “only” 100 to 1000, this would be invaluable. Although 3D plasmonic substrates are also available,⁹⁵ dielectric structures should offer more design flexibility in the third dimension (height), since they are much less absorbing.

On the important question of how to best quantify SERS EFs, here, we have touched on several crucial aspects but have not really provided a solution (because we do not have it yet). It is fair to say that there is still a need to develop a better “SERS EF standard” that the community could refer to when estimating SERS EF. From our earlier discussion, one should avoid resonant or even preresonant molecules. Reference 14, for example, recommended a few common (nonresonant) analytes. Further work is still needed to confirm their suitability as standards: studies at multiple excitation wavelengths, reproducibility across different laboratories, etc. In order to compare any experimental EF with theory, it will also be necessary to study in detail their CE and surface orientation properties. In parallel to choosing a SERS EF standard, we should also develop a standard operating procedure for measuring SERS EF (which should include a measure of the chosen analyte on the SERS substrate but also under well-defined normal conditions). Given the progress made over the years on all these aspects, this goal is now arguably within reach, but probably requires a concerted effort

from the SERS community. This would be invaluable for both SERS research and its many applications.

In closing, the examples discussed in this Perspective only provide a glimpse of the continued relevance of SERS EFs to the field, and SERS EFs will no doubt be featured prominently in the many possible future developments in the field.

AUTHOR INFORMATION

Corresponding Authors

Eric C. Le Ru – *The MacDiarmid Institute for Advanced Materials and Nanotechnology, School of Chemical and Physical Sciences, Victoria University of Wellington, Wellington 6140, New Zealand*; orcid.org/0000-0002-3052-9947; Email: eric.leru@vuw.ac.nz

Baptiste Auguie – *The MacDiarmid Institute for Advanced Materials and Nanotechnology, School of Chemical and Physical Sciences, Victoria University of Wellington, Wellington 6140, New Zealand*; Email: baptiste.auguie@vuw.ac.nz

Complete contact information is available at:

<https://pubs.acs.org/10.1021/acsnano.4c01474>

Notes

The authors declare no competing financial interest.

ACKNOWLEDGMENTS

This 50th anniversary of SERS also marks 10 years since our colleague Prof. Pablo Etchegoin passed away prematurely. As a large part of our work on SERS was carried out in close association with Pablo, it is timely to acknowledge again his enormous contribution to the field. E.C.L.R. acknowledges the support of the Royal Society Te Apārangi (New Zealand) through a Marsden Grant and of the MacDiarmid Institute for Advanced Materials and Nanotechnology. We thank C. Galloway and B. L. Darby for their help in acquiring the data of Figure 4.

REFERENCES

- (1) Fleischmann, M.; Hendra, P. J.; McQuillan, A. J. Raman spectra of pyridine adsorbed at a silver electrode. *Chem. Phys. Lett.* **1974**, *26*, 163–166.
- (2) Jeanmaire, D. L.; Van Duyne, R. P. Surface Raman spectroelectrochemistry. Part I. Heterocyclic, aromatic, and aliphatic amines adsorbed on the anodized silver electrode. *J. Electroanal. Chem.* **1977**, *84*, 1–20.
- (3) Albrecht, M. G.; Creighton, J. A. Anomalous intense Raman spectra of pyridine at a silver electrode. *J. Am. Chem. Soc.* **1977**, *99*, 5215–5217.
- (4) Le Ru, E. C.; Etchegoin, P. G. *Principles of Surface Enhanced Raman Spectroscopy and Related Plasmonic Effects*; Elsevier: Amsterdam, 2009.
- (5) Aroca, R. F. *Surface-Enhanced Vibrational Spectroscopy*; John Wiley & Sons: Chichester, U.K., 2006.
- (6) Langer, J.; Jimenez de Aberasturi, D.; Aizpurua, J.; Alvarez-Puebla, R. A.; Auguie, B.; Baumberg, J. J.; Bazan, G. C.; Bell, S. E. J.; Boisen, A.; Brolo, A. G.; et al. Present and Future of Surface-Enhanced Raman Scattering. *ACS Nano* **2020**, *14*, 28–117.
- (7) Moskovits, M. Surface roughness and the enhanced intensity of Raman scattering by molecules adsorbed on metals. *J. Chem. Phys.* **1978**, *69*, 4159–4161.
- (8) Moskovits, M.; Piorek, B. D. A brief history of surface-enhanced Raman spectroscopy and the localized surface plasmon Dedicated to the memory of Richard Van Duyne (1945–2019). *J. Raman Spectrosc.* **2021**, *52*, 279–284.
- (9) Le Ru, E. C.; Blackie, E.; Meyer, M.; Etchegoin, P. G. Surface Enhanced Raman Scattering enhancement factors: a comprehensive study. *J. Phys. Chem. C* **2007**, *111*, 13794–13803.

- (10) Baumberg, J. J. Picocavities: A Primer. *Nano Lett.* **2022**, *22*, 5859–5865.
- (11) Cortés, E.; Besteiro, L. V.; Alabastri, A.; Baldi, A.; Tagliabue, G.; Demetriadou, A.; Narang, P. Challenges in Plasmonic Catalysis. *ACS Nano* **2020**, *14*, 16202–16219.
- (12) Cialla-May, D.; Zheng, X.-S.; Weber, K.; Popp, J. Recent progress in surface-enhanced Raman spectroscopy for biological and biomedical applications: from cells to clinics. *Chem. Soc. Rev.* **2017**, *46*, 3945–3961.
- (13) Goodacre, R.; Graham, D.; Faulds, K. Recent developments in quantitative SERS: Moving towards absolute quantification. *Trends Anal. Chem.* **2018**, *102*, 359–368.
- (14) Bell, S. E. J.; Charron, G.; Cortés, E.; Kneipp, J.; de la Chapelle, M. L.; Langer, J.; Procházka, M.; Tran, V.; Schlücker, S. Towards Reliable and Quantitative Surface-Enhanced Raman Scattering (SERS): From Key Parameters to Good Analytical Practice. *Angew. Chem., Int. Ed.* **2020**, *59*, 5454–5462.
- (15) Le Ru, E. C.; Etchegoin, P. G. Quantifying SERS enhancements. *MRS Bull.* **2013**, *38*, 631–640.
- (16) Le Ru, E. C.; Etchegoin, P. G. Rigorous Justification of the $|E|^4$ Enhancement Factor in Surface Enhanced Raman Spectroscopy. *Chem. Phys. Lett.* **2006**, *423*, 63–66.
- (17) Lombardi, J. R.; Birke, R. L.; Lu, T.; Xu, J. Charge transfer theory of surface enhanced Raman spectroscopy; Herzberg-Teller contributions. *J. Chem. Phys.* **1986**, *84*, 4174–4180.
- (18) Lombardi, J. R.; Birke, R. L. A unified approach to surface-enhanced Raman spectroscopy. *J. Phys. Chem. C* **2008**, *112*, 5605–5617.
- (19) Valley, N.; Greeneltch, N.; Van Duyne, R. P.; Schatz, G. C. A Look at the Origin and Magnitude of the Chemical Contribution to the Enhancement Mechanism of Surface-Enhanced Raman Spectroscopy (SERS): Theory and Experiment. *J. Phys. Chem. Lett.* **2013**, *4*, 2599–2604.
- (20) Morton, S. M.; Jensen, L. Understanding the Molecule–Surface Chemical Coupling in SERS. *J. Am. Chem. Soc.* **2009**, *131*, 4090–4098.
- (21) Li, J. F.; Huang, Y. F.; Ding, Y.; Yang, Z. L.; Li, S. B.; Zhou, X. S.; Fan, F. R.; Zhang, W.; Zhou, Z. Y.; Wu, D. Y.; Ren, B.; Wang, Z. L.; Tian, Z. Q. Shell-isolated nanoparticle-enhanced Raman spectroscopy. *Nature* **2010**, *464*, 392–395.
- (22) Le Ru, E. C.; Etchegoin, P. G.; Meyer, M. Enhancement factor distribution around a single SERS hot-spot and its relation to single molecule detection. *J. Chem. Phys.* **2006**, *125*, 204701.
- (23) Fang, Y.; Seong, N.-H.; Dlott, D. D. Measurement of the distribution of site enhancements in surface-enhanced Raman scattering. *Science* **2008**, *321*, 388–391.
- (24) Le Ru, E. C.; Meyer, M.; Etchegoin, P. G. Proof of Single-Molecule Sensitivity in Surface Enhanced Raman Scattering (SERS) by Means of a Two-Analyte Technique. *J. Phys. Chem. B* **2006**, *110*, 1944–1948.
- (25) Wustholz, K. L.; Henry, A.-I.; McMahon, J. M.; Freeman, R. G.; Valley, N.; Piotti, M. E.; Natan, M. J.; Schatz, G. C.; Van Duyne, R. P. Structure–Activity Relationships in Gold Nanoparticle Dimers and Trimers for Surface-Enhanced Raman Spectroscopy. *J. Am. Chem. Soc.* **2010**, *132*, 10903–10910.
- (26) Kusch, P.; Mastel, S.; Mueller, N. S.; Morquillas Azpiazu, N.; Heeg, S.; Gorbachev, R.; Schedin, F.; Hübner, U.; Pascual, J. I.; Reich, S.; Hillenbrand, R. Dual-Scattering Near-Field Microscope for Correlative Nanoimaging of SERS and Electromagnetic Hotspots. *Nano Lett.* **2017**, *17*, 2667–2673.
- (27) Le Ru, E. C.; Etchegoin, P. G. Single molecule surfaced-enhanced Raman spectroscopy. *Annu. Rev. Phys. Chem.* **2012**, *63*, 65.
- (28) dos Santos, D. P.; Temperini, M. L. A.; Brolo, A. G. Intensity Fluctuations in Single-Molecule Surface-Enhanced Raman Scattering. *Acc. Chem. Res.* **2019**, *52*, 456–464.
- (29) Dieringer, J. A.; Lettan, R. B., II; Scheidt, K. A.; Van Duyne, R. P. A frequency domain existence proof of single-molecule surface-enhanced Raman Spectroscopy. *J. Am. Chem. Soc.* **2007**, *129*, 16249–16256.
- (30) Blackie, E.; Le Ru, E. C.; Meyer, M.; Timmer, M.; Burkett, B.; Northcote, P.; Etchegoin, P. G. Bi-analyte SERS with isotopically edited dyes. *Phys. Chem. Chem. Phys.* **2008**, *10*, 4147–4153.
- (31) Park, J.-E.; Lee, Y.; Nam, J.-M. Precisely Shaped, Uniformly Formed Gold Nanocubes with Ultrahigh Reproducibility in Single-Particle Scattering and Surface-Enhanced Raman Scattering. *Nano Lett.* **2018**, *18*, 6475–6482.
- (32) Pettinger, B.; Schambach, P.; Villagómez, C. J.; Scott, N. Tip-Enhanced Raman Spectroscopy: Near-Fields Acting on a Few Molecules. *Annu. Rev. Phys. Chem.* **2012**, *63*, 379–399.
- (33) Zhang, R.; Zhang, Y.; Dong, Z. C.; Jiang, S.; Zhang, C.; Chen, L. G.; Zhang, L.; Liao, Y.; Aizpurua, J.; Luo, Y.; Yang, J. L.; Hou, J. G. Chemical mapping of a single molecule by plasmon-enhanced Raman scattering. *Nature* **2013**, *498*, 82–86.
- (34) Jiang, S.; Zhang, Y.; Zhang, R.; Hu, C.; Liao, M.; Luo, Y.; Yang, J.; Dong, Z.; Hou, J. G. Distinguishing adjacent molecules on a surface using plasmon-enhanced Raman scattering. *Nat. Nanotechnol.* **2015**, *10*, 865–869.
- (35) Chiang, N.; Chen, X.; Goubert, G.; Chulhai, D. V.; Chen, X.; Pozzi, E. A.; Jiang, N.; Hersam, M. C.; Seideman, T.; Jensen, L.; Van Duyne, R. P. Conformational Contrast of Surface-Mediated Molecular Switches Yields Ångstrom-Scale Spatial Resolution in Ultrahigh Vacuum Tip-Enhanced Raman Spectroscopy. *Nano Lett.* **2016**, *16*, 7774–7778.
- (36) Benz, F.; Schmidt, M. K.; Dreismann, A.; Chikkaraddy, R.; Zhang, Y.; Demetriadou, A.; Carnegie, C.; Ohadi, H.; de Nijs, B.; Esteban, R.; Aizpurua, J.; Baumberg, J. J. Single-molecule optomechanics in “picocavities”. *Science* **2016**, *354*, 726–729.
- (37) Shin, H.-H.; Yeon, G. J.; Choi, H.-K.; Park, S.-M.; Lee, K. S.; Kim, Z. H. Frequency-Domain Proof of the Existence of Atomic-Scale SERS Hot-Spots. *Nano Lett.* **2018**, *18*, 262–271.
- (38) Peng, W.; Zhou, J.-W.; Li, M.-L.; Sun, L.; Zhang, Y.-J.; Li, J.-F. Construction of nanoparticle-on-mirror nanocavities and their applications in plasmon-enhanced spectroscopy. *Chem. Sci.* **2024**, *15*, 2697–2711.
- (39) Trautmann, S.; Aizpurua, J.; Götz, I.; Undisz, A.; Dellith, J.; Schneidewind, H.; Rettenmayr, M.; Deckert, V. A classical description of subnanometer resolution by atomic features in metallic structures. *Nanoscale* **2017**, *9*, 391–401.
- (40) Urbieto, M.; Barbry, M.; Zhang, Y.; Koval, P.; Sánchez-Portal, D.; Zabala, N.; Aizpurua, J. Atomic-Scale Lightning Rod Effect in Plasmonic Picocavities: A Classical View to a Quantum Effect. *ACS Nano* **2018**, *12*, 585–595.
- (41) Auguie, B.; Reigue, A.; Le Ru, E. C.; Etchegoin, P. G. Tiny Peaks vs Mega Backgrounds: A General Spectroscopic Method with Applications in Resonant Raman Scattering and Atmospheric Absorptions. *Anal. Chem.* **2012**, *84*, 7938.
- (42) Xu, H.; Bjerneld, E. J.; Käll, M.; Börjesson, L. Spectroscopy of single hemoglobin molecules by surface enhanced Raman scattering. *Phys. Rev. Lett.* **1999**, *83*, 4357–4360.
- (43) Blackie, E. J.; Le Ru, E. C.; Etchegoin, P. G. Single molecule surface-enhanced Raman spectroscopy of non-resonant molecules. *J. Am. Chem. Soc.* **2009**, *131*, 14466–14472.
- (44) Kneipp, K.; Wang, Y.; Kneipp, H.; Perelman, L. T.; Itzkan, I.; Dasari, R. R.; Feld, M. S. Single molecule detection using surface-enhanced Raman scattering (SERS). *Phys. Rev. Lett.* **1997**, *78*, 1667–1670.
- (45) Nie, S.; Emory, S. R. Probing single molecules and single nanoparticles by surface-enhanced Raman scattering. *Science* **1997**, *275*, 1102–1106.
- (46) Kleinman, S. L.; Sharma, B.; Blaber, M. G.; Henry, A.-I.; Valley, N.; Freeman, R. G.; Natan, M. J.; Schatz, G. C.; Van Duyne, R. P. Structure Enhancement Factor Relationships in Single Gold Nanoparticles by Surface-Enhanced Raman Excitation Spectroscopy. *J. Am. Chem. Soc.* **2013**, *135*, 301–308.
- (47) Henry, A.-I.; Ueltschi, T. W.; McAnally, M. O.; Van Duyne, R. P. Spiers Memorial Lecture Surface-enhanced Raman spectroscopy: from single particle/molecule spectroscopy to Ångstrom-scale spatial

resolution and femtosecond time resolution. *Faraday Discuss.* **2017**, *205*, 9–30.

(48) Le Ru, E. C.; Meyer, S. A.; Artur, C.; Etchegoin, P. G.; Grand, J.; Lang, P.; Maurel, F. Experimental demonstration of surface selection rules for SERS on flat metallic surfaces. *Chem. Commun.* **2011**, *47*, 3903–3905.

(49) Moskovits, M. Surface selection rules. *J. Chem. Phys.* **1982**, *77*, 4408–4416.

(50) Maher, R. C.; Galloway, C. M.; Le Ru, E. C.; Cohen, L. F.; Etchegoin, P. G. Vibrational pumping in surface enhanced Raman scattering (SERS). *Chem. Soc. Rev.* **2008**, *37*, 965–979.

(51) Galloway, C. M.; Le Ru, E. C.; Etchegoin, P. G. Single-molecule vibrational pumping in SERS. *Phys. Chem. Chem. Phys.* **2009**, *11*, 7372–7380.

(52) Darby, B. D.; Etchegoin, P. G.; Le Ru, E. C. Single-molecule surface-enhanced Raman spectroscopy with nanowatt excitation. *Phys. Chem. Chem. Phys.* **2014**, *16*, 23895.

(53) Le Ru, E. C.; Schroeter, L. C.; Etchegoin, P. G. Direct Measurement of Resonance Raman Spectra and Cross Sections by a Polarization Difference Technique. *Anal. Chem.* **2012**, *84*, 5074.

(54) Xu, F.; Zhang, Y.; Sun, Y.; Shi, Y.; Wen, Z.; Li, Z. Silver Nanoparticles Coated Zinc Oxide Nanorods Array as Superhydrophobic Substrate for the Amplified SERS Effect. *J. Phys. Chem. C* **2011**, *115*, 9977–9983.

(55) De Angelis, F.; Gentile, F.; Mecarini, F.; Das, G.; Moretti, M.; Candeloro, P.; Coluccio, M. L.; Cojoc, G.; Accardo, A.; Liberale, C.; Zaccaria, R. P.; Perozziello, G.; Tirinato, L.; Toma, A.; Cuda, G.; Cingolani, R.; Di Fabrizio, E. Breaking the diffusion limit with superhydrophobic delivery of molecules to plasmonic nanofocusing SERS structures. *Nat. Photonics* **2011**, *5*, 682–687.

(56) Fan, M.; Cheng, F.; Wang, C.; Gong, Z.; Tang, C.; Man, C.; Brolo, A. G. SERS optrode as a “fishing rod” to direct pre-concentrate analytes from superhydrophobic surfaces. *Chem. Commun.* **2015**, *51*, 1965–1968.

(57) Wallace, R. A.; Charlton, J. J.; Kirchner, T. B.; Lavrik, N. V.; Datskos, P. G.; Sepaniak, M. J. Superhydrophobic Analyte Concentration Utilizing Colloid-Pillar Array SERS Substrates. *Anal. Chem.* **2014**, *86*, 11819–11825.

(58) Song, W.; Psaltis, D.; Crozier, K. B. Superhydrophobic bull’s-eye for surface-enhanced Raman scattering. *Lab Chip* **2014**, *14*, 3907–3911.

(59) Leyton, P.; Sanchez-Cortes, S.; Campos-Vallette, M.; Domingo, C.; Garcia-Ramos, J. V.; Saitz, C. Surface-enhanced micro-Raman detection and characterization of calix[4]arene-polycyclic aromatic hydrocarbon host-guest complexes. *Appl. Spectrosc.* **2005**, *59*, 1009–1015.

(60) Stewart, A.; Murray, S.; Bell, S. E. J. Simple preparation of positively charged silver nanoparticles for detection of anions by surface-enhanced Raman spectroscopy. *Analyst* **2015**, *140*, 2988–2994.

(61) Chen, T.; Du, C.; Tan, L. H.; Shen, Z.; Chen, H. Site-selective localization of analytes on gold nanorod surface for investigating field enhancement distribution in surface-enhanced Raman scattering. *Nanoscale* **2011**, *3*, 1575–1581.

(62) Lee, A.; Andrade, G. F. S.; Ahmed, A.; Souza, M. L.; Coombs, N.; Tumarkin, E.; Liu, K.; Gordon, R.; Brolo, A. G.; Kumacheva, E. Probing Dynamic Generation of Hot-Spots in Self-Assembled Chains of Gold Nanorods by Surface-Enhanced Raman Scattering. *J. Am. Chem. Soc.* **2011**, *133*, 7563–7570.

(63) Le Ru, E. C.; Grand, J.; Sow, I.; Somerville, W. R. C.; Etchegoin, P. G.; Treguer-Delapierre, M.; Charron, G.; Felidj, N.; Levi, G.; Aubard, J. A scheme for detecting every single target molecule with Surface-Enhanced Raman Spectroscopy. *Nano Lett.* **2011**, *11*, 5013.

(64) Darby, B. L.; Auguie, B.; Meyer, M.; Pantoja, A. E.; Le Ru, E. C. Modified Optical Absorption of Molecules on Metallic Nanoparticles at Sub-Monolayer Coverage. *Nat. Photonics* **2016**, *10*, 40.

(65) Page, J. B.; Tonks, D. On the separation of resonance Raman scattering into orders in the time correlator theory. *J. Chem. Phys.* **1981**, *75*, 5694–5708.

(66) Brafman, O.; Chan, C.; Khodadoost, B.; Page, J.; Walker, C. Resonance Raman scattering study of azulene. I. experiment and theoretical analysis via transform techniques. *J. Chem. Phys.* **1984**, *80*, 5406–5417.

(67) Meyer, S. A.; Le Ru, E. C.; Etchegoin, P. G. Quantifying Resonant Raman Cross Sections with SERS. *J. Phys. Chem. A* **2010**, *114*, 5515–5519.

(68) Darby, B. L. *Probing the interactions between dye molecules and metallic nanoparticles—Implications for surface enhanced spectroscopies*; Ph.D. Thesis, Victoria University of Wellington, 2016.

(69) Stefanu, A.; Gargiulo, J.; Laufersky, G.; Auguie, B.; Chiş, V.; Le Ru, E. C.; Liu, M.; Leopold, N.; Cortés, E. Interface-Dependent Selectivity in Plasmon-Driven Chemical Reactions. *ACS Nano* **2023**, *17*, 3119.

(70) Dieringer, J. A.; Wustholz, K. L.; Masiello, D. J.; Camden, J. P.; Kleinman, S. L.; Schatz, G. C.; Van Duyne, R. P. Surface-Enhanced Raman Excitation Spectroscopy of a Single Rhodamine 6G Molecule. *J. Am. Chem. Soc.* **2009**, *131*, 849–854.

(71) Petráková, V.; Sampaio, I. C.; Reich, S. Optical Absorption of Dye Molecules Remains Unaffected by Submonolayer Complex Formation with Metal Nanoparticles. *J. Phys. Chem. C* **2019**, *123*, 17498–17504.

(72) Auguie, B.; Darby, B. L.; Le Ru, E. C. Electromagnetic interactions of dye molecules surrounding a nanosphere. *Nanoscale* **2019**, *11*, 12177–12187.

(73) Khlebtsov, N. G.; Le Ru, E. C. Analytical solutions for the surface- and orientation-averaged SERS enhancement factor of small plasmonic particles. *J. Raman Spectrosc.* **2021**, *52*, 285–295.

(74) Le Ru, E. C.; Grand, J.; Felidj, N.; Aubard, J.; Lévi, G.; Hohenau, A.; Krenn, J. R.; Blackie, E.; Etchegoin, P. G. Experimental verification of the SERS electromagnetic model beyond the $|E|^4$ approximation: Polarization Effects. *J. Phys. Chem. C* **2008**, *112*, 8117–8121.

(75) Le Ru, E. C.; Meyer, M.; Blackie, E.; Etchegoin, P. G. Advanced aspects of electromagnetic SERS enhancement factors at a hot-spot. *J. Raman Spectrosc.* **2008**, *39*, 1127–1134.

(76) McLellan, J. M.; Li, Z.-Y.; Siekkinen, A. R.; Xia, Y. The SERS Activity of a Supported Ag Nanocube Strongly Depends on Its Orientation Relative to Laser Polarization. *Nano Lett.* **2007**, *7*, 1013–1017.

(77) Stranahan, S. M.; Titus, E. J.; Willets, K. A. SERS Orientational Imaging of Silver Nanoparticle Dimers. *J. Phys. Chem. Lett.* **2011**, *2*, 2711–2715.

(78) Le Ru, E. C.; Etchegoin, P. G. *SERS and Plasmonics Codes (SPLaC)*. Matlab codes freely available from <http://www.vuw.ac.nz/raman/book/codes.aspx>, 2009 (last accessed Dec. 1, 2020).

(79) Kneipp, K.; Wang, Y.; Kneipp, H.; Itzkan, I.; Dasari, R. R.; Feld, M. S. Population Pumping of Excited Vibrational States by Spontaneous Surface-Enhanced Raman Scattering. *Phys. Rev. Lett.* **1996**, *76*, 2444–2447.

(80) Roelli, P.; Galland, C.; Piro, N.; Kippenberg, T. J. Molecular cavity optomechanics as a theory of plasmon-enhanced Raman scattering. *Nat. Nanotechnol.* **2016**, *11*, 164–169.

(81) Le Ru, E. C.; Etchegoin, P. G. Vibrational pumping and heating under SERS conditions: fact or myth? *Faraday Discuss.* **2006**, *132*, 63–75.

(82) Maher, R. C.; Cohen, L. F.; Le Ru, E. C.; Etchegoin, P. G. On the Experimental Estimation of Surface Enhanced Raman Scattering (SERS) Cross Sections by Vibrational Pumping. *J. Phys. Chem. B* **2006**, *110*, 19469–19478.

(83) Gill, R.; Tian, L.; Somerville, W. R. C.; Le Ru, E. C.; van Amerongen, H.; Subramaniam, V. Silver Nanoparticle Aggregates as Highly Efficient Plasmonic Antennas for Fluorescence Enhancement. *J. Phys. Chem. C* **2012**, *116*, 16687.

(84) Galloway, C. M.; Etchegoin, P. G.; Le Ru, E. C. Ultrafast nonradiative decay rates on metallic surfaces by comparing surface-enhanced Raman and fluorescence signals of single molecules. *Phys. Rev. Lett.* **2009**, *103*, 063003.

- (85) Le Ru, E. C.; Etchegoin, P. G.; Grand, J.; Félidj, N.; Aubard, J.; Lévi, G. The mechanisms of spectral profile modification in surface enhanced fluorescence. *J. Phys. Chem. C* **2007**, *111*, 16076–16079.
- (86) Le Ru, E. C.; Etchegoin, P. G.; Grand, J.; Félidj, N.; Aubard, J.; Lévi, G.; Hohenau, A.; Krenn, J. Surface enhanced Raman spectroscopy on nanolithography-prepared substrates. *Cur. Appl. Phys.* **2008**, *8*, 467–470.
- (87) Lin, K.-Q.; Yi, J.; Zhong, J.-H.; Hu, S.; Liu, B.-J.; Liu, J.-Y.; Zong, C.; Lei, Z.-C.; Wang, X.; Aizpurua, J.; Esteban, R.; Ren, B.; et al. Plasmonic photoluminescence for recovering native chemical information from surface-enhanced Raman scattering. *Nat. Commun.* **2017**, *8*, 14891.
- (88) Zhang, Y.; Guo, W.; Zhang, Y.; Wei, W. D. Plasmonic Photoelectrochemistry: In View of Hot Carriers. *Adv. Mater.* **2021**, *33*, 2006654.
- (89) Kamarudheen, R.; Aalbers, G. J. W.; Hamans, R. F.; Kamp, L. P. J.; Baldi, A. Distinguishing Among All Possible Activation Mechanisms of a Plasmon-Driven Chemical Reaction. *ACS Energy Lett.* **2020**, *5*, 2605–2613.
- (90) Movsesyan, A.; Santiago, E. Y.; Burger, S.; Correa-Duarte, M. A.; Besteiro, L. V.; Wang, Z.; Govorov, A. O. Plasmonic Nanocrystals with Complex Shapes for Photocatalysis and Growth: Contrasting Anisotropic Hot-Electron Generation with the Photothermal Effect. *Adv. Opt. Mater.* **2022**, *10*, 2102663.
- (91) Arul, R.; Menghrajani, K.; Rider, M. S.; Chikkaraddy, R.; Barnes, W. L.; Baumberg, J. J. Raman Probing the Local Ultrastrong Coupling of Vibrational Plasmon Polaritons on Metallic Gratings. *Phys. Rev. Lett.* **2023**, *131*, 126902.
- (92) Galloway, C. M.; Artur, C.; Grand, J.; Le Ru, E. C. Photobleaching of Fluorophores on the Surface of Nanoantennas. *J. Phys. Chem. C* **2014**, *118*, 28820–28830.
- (93) Caldarola, M.; Albella, P.; Cortés, E.; Rahmani, M.; Roschuk, T.; Grinblat, G.; Oulton, R. F.; Bragas, A. V.; Maier, S. A. Non-plasmonic nanoantennas for surface enhanced spectroscopies with ultra-low heat conversion. *Nat. Commun.* **2015**, *6*, 7915.
- (94) Hu, S.; Khater, M.; Salas-Montiel, R.; Kratschmer, E.; Engelmann, S.; Green, W. M. J.; Weiss, S. M. Experimental realization of deep-subwavelength confinement in dielectric optical resonators. *Sci. Adv.* **2018**, *4*, eaat2355.
- (95) Han, Y.; Wu, S.-R.; Tian, X.-D.; Zhang, Y. Optimizing the SERS Performance of 3D Substrates through Tunable 3D Plasmonic Coupling toward Label-Free Liver Cancer Cell Classification. *ACS Appl. Mater. Interface* **2020**, *12*, 28965–28974.